JOURNAL OF MATERIALS SCIENCE **34** (1999) 1163–1167

Preparation and characterization of perovskite ceramic powders by gelcasting

HUANTING WANG†, SONG XIE, WEI LAI, XINGQIN LIU, CHUSHENG CHEN, GUANGYAO MENG*
Department of Materials Science and Engineering, University of Science and Technology of China, Hefei, Anhui, 230026, People's Republic of China

Perovskite $La_{0.6}Sr_{0.4}Co_{0.8}Fe_{0.2}O_{3-\delta}$ (LSCF) powders have been successfully synthesized from oxide and carbonates based on the principle of gelcasting. Phase-forming temperature is very dependent on the ball-milling process during the suspension preparation. As the ball-milling time is increased, the temperature of phase formation decreases, therefore the perovskite powder obtained has a larger Brunaver–Emmett–Teller (BET) specific surface area. The grain sizes were around 1 μm at 1000 °C and 2 μm at 1100 °C from scanning electron microscopy (SEM) photographs. The perovskite powders have good sinterability: the sintering densities of ceramic bodies shaped with as-prepared powders were investigated. SEM photos show that sintered ceramics exhibit a well defined morphology in the packing and sintering of particles. The oxygen permeance of disc shaped samples, with a thickness ranging from 1.02 to 1.98 mm was 6.39×10^{-8}–1.99×10^{-8} mol cm^{-2} s^{-1} at 900 °C indicating that LSCF ceramics have high oxygen permeation. It can be concluded that gelcasting is a simple and effective method for preparing practical multicomponent perovskite powders.

1. Introduction

Perovskite-type (ABO_3) oxides have been extensively studied for many technical applications, such as in: catalysis [1], high temperature ceramic superconductors [2], and electronics [3]. Furthermore, they are selected as electrodes for solid oxide fuel cells (SOFC) [4] and oxygen gas separation membranes [5] because of their oxygen-sorptive and electronic conductive properties. Generally, perovskite ceramics are fabricated from perovskite powders, which are synthesized by a conventional solid state reaction method as well as wet chemical processes, including thermal decomposition of cyanide [6], hydroxides, metal-EDTA- [7] and oxalic complexes, chemical coprecipitation and the sol–gel process [8]. The gelcasting process, which has been developed for the production of complex-shaped parts [9], has been introduced to prepare perovskite ceramics from metal oxide and its precursors [10]. This method is very suitable for preparing porous perovskite ceramics, however, a large linear shrinkage of 28.5% is produced when dense ceramics are obtained because thermal decomposition of reactive species takes place during reaction-sintering, this may lead to defects, such as cracks, deformation, etc. If the ceramic body is fabricated from perovskite powders, which can also be synthesized from metal oxide and its precursors, sintering shrinkage will significantly decrease, and therefore some defects may be avoided.

Based on our previous work, perovskite $La_{0.6}Sr_{0.4}Co_{0.8}Fe_{0.2}O_{3-\delta}$ (LSCF) with high oxygen ionic and electronic conductivity [5] is used here to illustrate powder preparation from insoluble or low-solubility metal precursors, based on the principle of gelcasting, and powder characterization so as to examine the applicability of the preparation method used in this work.

2. Experimental procedure

2.1. Synthesis of perovskite powder

The starting materials were lanthanum (La_2O_3), strontium carbonate ($SrCO_3$), basic cobalt carbonate ($2CoCO_3 \cdot 3Co(OH)_2 \cdot xH_2O$) and iron oxide ($Fe_2O_3$). $2CoCO_3 \cdot 3Co(OH)_2 \cdot xH_2O$ is very hygroscopic, and in this experiment the crystal water content, x, is 6.14 from thermogravimetric analysis (TGA). The chemicals, mixed in aqueous monomer [acrylamide, AM and N,N′-methylenebis-acrylamide, MBAM, AM : MBAM 20 : 1 (by weight)] solution with a concentration of 10 wt % in stoichiometric ratio of LSCF, were ball-milled for different times. The resulting slurry, with the initiator ammonium bisulphate $(NH_4)_2S_2O_8$ (1.6 wt % of organic monomers) and a little catalyst N,N,N′,N′-tetramethylethylenediamine (TEMED), was cast into a mould and solidified about 30 min later. The dried gelcasts were fast dried in an oven at 100 °C and calcined

† *Present address*: Division of Chemistry and Chemical Engineering 210-41, California Institute of Technology, Pasadena, CA 91125, USA.
* Corresponding author email: mgym@ustc.edu.cn

at 2 °C min^{-1}. The calcined samples were ground into powders.

2.2. Characterization

2.2.1. Powder formation

Simultaneous differential thermal analysis and thermogravimetry (DTA–TGA) were carried out on the dried gelcasts obtained using a thermal analyser (Netzsch STA 429). Samples were heated from 25 to 1300 °C at a heating rate of 1 °C min^{-1} under dynamic air flow.

The gelcasts sintered in static air for 8 h from 800 to 1300 °C were characterized by X-ray diffraction (XRD) and primary crystal sizes were calculated.

Brunaver–Emmett–Teller (BET) specific surface area of ground powders was measured (Micromeritics ASAP 2000).

Microstructure characterization of all specimens was carried out on a Hitachi X-650 scanning electronic microscope (SEM).

2.2.2. Sintering property of perovskite powder

The sinterability of powders is very important for fabricating useful ceramics. The as-prepared powders were used to fabricate a ceramic body by gelcasting as described above. The slurry was dispersed by stirring in place of ball-milling because of the small amount of slurry. The wet ceramic body was dried in an oven at 50 °C. The dried ceramic bodies were machined and finished to discs of diameter 25 × 2 mm in thickness, and then sintered in a programmable high temperature furnace (Nabertherm, Germany) under different conditions in order to investigate their sintering behaviour based on the change of relative density of sintered specimens obtained by the Archimedes' method (a theoretical density of 6.448 g cm^{-3} for LSCF).

2.2.3. Oxygen permeation measurement

The powder can be further characterized by measuring the oxygen permeation of the ceramics obtained. The sintered discs were ground to 12 mm in diameter, their both sides were polished with emery paper before use. The oxygen permeation were measured with the apparatus described in the literature [5] at a temperature range of 900–1100 °C. The disc membrane was supported by a dense alumina tube, a glass O-ring was placed between the disc and the alumina tube to construct the sample cell, which was put into a vertical-type electric furnace with a programmable temperature controller. When measuring, the sample cell was heated up to 1150 °C thus melting the glass ring to ensure the gas tightness of the cell. With one side of the disc being exposed to air, the other side was exposed to a flow of helium (flow rate 35.92 cm^3 min^{-1}). Under this condition, the disc from the air side to helium side at respective temperatures was detected by gas chromatography (GC).

3. Results and discussion

3.1. Thermal decomposition of gelcast body

DTA–TGA were used in analysing the thermal decomposition of the gelcast body. Fig. 1 shows the DTA–TGA results of the gelcast in air. At $T < 240$ °C, there is approximately 9% mass loss, which is caused by endothermic removal of crystal water of $2CoCO_3 \cdot 3Co(OH)_2 \cdot xH_2O$ and occluded water of the polymer network in gelcast specimens. In the temperature range 240–350 °C, there is a mass loss for the specimen accompanied by a large exothermic DTA peak, this attributes to the burn-out of the crosslinked polymer network. At approximately 700 °C, another mass loss starts, which is complete at approximately 920 °C. This is ascribed to the thermal decomposition of $SrCO_3$ and $2CoCO_3 \cdot 3Co(OH)_2$ due to solid state reaction among carbonates and oxides and the formation of an LSCF perovskite phase, as evidenced by XRD. No apparent mass loss occurs at $T > 920$ °C, indicating the decomposition of $SrCO_3$ and $2CoCO_3 \cdot 3Co(OH)_2$ is complete.

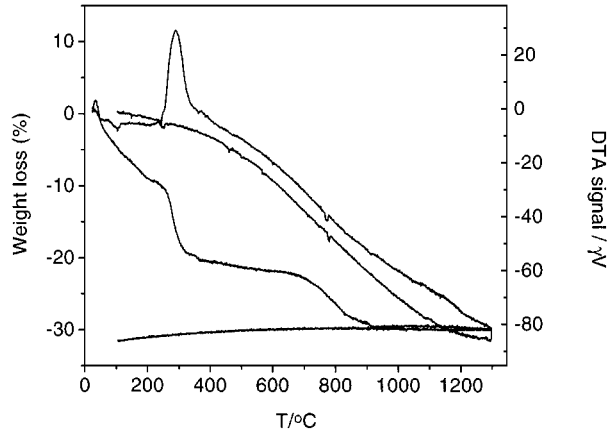

Figure 1 DTA and TGA curves of the gelcast body prepared from oxide and carbonate powders.

3.2. Effect of ball-milling time on temperature of phase formation

The LSCF gelcasts were sintered between 800 and 1300 °C, at 100 °C intervals, for 8 h, and the products were identified by XRD. At 800 °C, only carbonate and oxide were present and no perovskite phase was formed for specimens. The effect of ball-milling time on phase-forming temperature is listed in Table I. When the temperature was raised to 900 °C, the solid state reaction led to the formation of a perovskite phase, with a corresponding decrease in carbonate and oxide phases. At this temperature and at a ball-milling time greater than 48 h, a pure perovskite phase formed. Only when the ball-milling time was 10 h did a complete perovskite

TABLE I Formation of perovskite phase[a,b] identified by XRD

	Calcining temperature (°C)		
Ball-milling time (h)	900	1000	1100
5	−	−	+
10	−	+	+
24	−	+	+
48	+	+	+
72	+	+	+

[a] +, pure perovskite phase.
[b] −, non-pure phase.

phase form at 1000 °C. However, as the firing temperature reached 1100 °C, a perovskite LSCF phase could be obtained following ball-milling for 5 h. Phase formation is dependent not only on the firing temperature, but strongly on the ball-milling time; this is because the starting materials were more finely ground in size with increased duration of ball-milling (obviously, smaller reactive species have higher reactivity to present the results in our case). When the firing temperature was further raised to 1300 °C, specimens formed and retained the perovskite phase. All perovskite-type specimens exhibited a metallic luster to some extent. The XRD pattern of a typical perovskite phase from a LSCF gelcast is shown in [10].

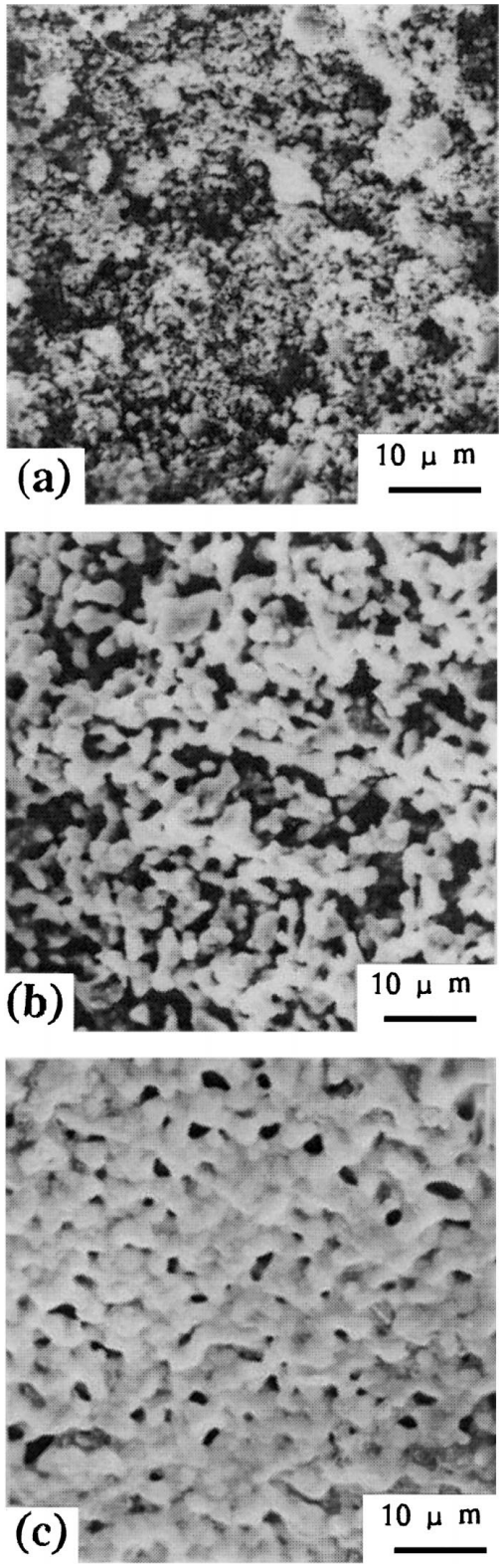

Figure 2 Scanning electron micrographs of gelcasts prepared from carbonate and oxide powders calcined at different temperatures: (a) uncalcined LSCF gelcast body ball-milled for 48 h, (b) perovskite LSCF calcined at 1000 °C for 6 h, and (c) perovskite LSCF calcined at 1100 °C for 6 h.

3.3. Microstructure of the gelcast body

SEM photographs of the fracture surfaces of uncalcined and calcined gelcasts with pure perovskite phase are shown in Fig. 2. From Fig. 2a, it can be seen that there are homogeneous submicrometre-sized particles immobilized by the crosslinked polymer network in the dried gelcast body, which are ideal for consequent solid state reaction. While solid state reaction occurred, grains with a perovskite phase grew with firing temperature. The grain sizes are around 1 μm at 1000 °C and 2 μm at 1100 °C, as shown in Fig. 2 (b, c).

3.4. BET specific surface areas of ground powders

Table II lists the results of BET specific surface area and primary crystal size of ground powders from gelcasts ball-milled for 48 h. As firing temperature increased, primary crystal size increased, meanwhile sintering of grains took place leading to grind difficulty, therefore the BET specific surface area of the ground powders decreased.

3.5. Sintering of perovskite ceramic powders

Powder B was used to prepare dense ceramic by gelcasting. The ceramic bodies were sintered at 1150, 1250 and 1300 °C for different times to observe the sintering behaviour. Sintering temperature and time dependence of the relative density is shown in Fig. 3. Sintering was very dependent on temperature, e.g. the relative density only reached 70% at 1150 °C for 25 h, and it could reach more than 90% at 1250 °C. It could also be seen that sintering equilibrium needed a short time as the temperature was high. In our case the relative density of the perovskite ceramics slightly decreased at 1250 °C or greater. Generally, there were a few closed pores in the samples sintered at 1250 °C. This could be further proven from the microstructure of samples sintered at 1150, 1250 and 1300 °C for 6 h shown in Fig. 4. With increased sintering temperature, pores in samples decreased and almost disappeared fully at 1300 °C. It could also be found that sintered specimens exhibited

TABLE II BET specific surface areas and primary crystal sizes of ground powders from gelcasts ball-milled for 48 h

Sample No.	T_{calc} (°C)	S_{BET} ($m^2\ g^{-1}$)	Primary crystal size (nm)
A	900	4.6033	24
B	1000	4.4895	27
C	1100	1.7048	43

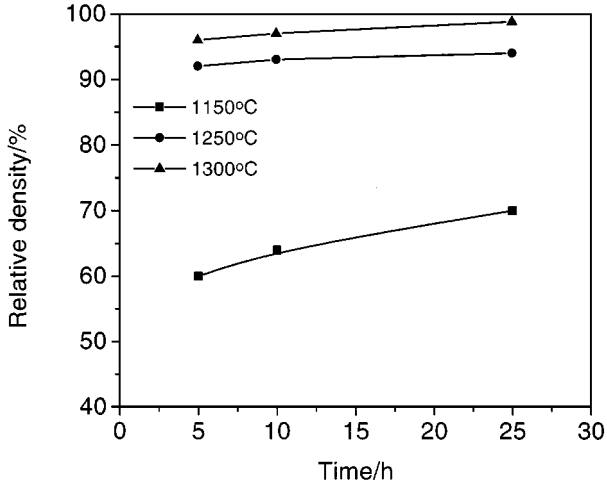

Figure 3 Sintering temperature and time dependence of relative density.

a well defined morphology in the packing and sintering of particles, which may provide high mechanical strength.

3.6. Oxygen permeance of sintered ceramics

Disc shaped samples sintered at 1300 °C for 6 h were used to measure oxygen permeation. It should be mentioned that a small steady nitrogen flow was detected, while a large amount of oxygen permeated during the entire experiment, shown in Fig. 5. The possible reasons were sealing leakage and/or sample defects. The latter may be ascribed to microcracks and micropores of sintered ceramics produced by a heterogeneous polymer of ceramic bodies, because of poor dispersion of the slurry by stirring. This will be further investigated in future work. In this paper oxygen permeance of the samples was obtained by subtracting leakage flow. The temperature variation of the oxygen permeation rate from the air to the helium side of the samples is shown in Fig. 6. The oxygen permeance of samples with respective thicknesses of 1.02 and 1.98 mm was 6.39×10^{-8} and 1.99×10^{-8} mol cm^{-2} s^{-1} at 900 °C. When Fig. 6 was transferred into log jo_2 versus $1000/T$, as shown in Fig. 7, the activation energy E_a, of oxygen permeation could be calculated to be 102.5 and 102.6 kJ mol^{-1}, respectively. This implies that the activation energy of oxygen permeation for LSCF with a thickness range of 1.02–1.98 mm is not strongly dependent on the membrane thickness. These data are of the same magnitude as the oxygen permeance values of 6.25×10^{-8} and 5.33×10^{-8} mol cm^{-2} s^{-1}, giving activation energies of 128 and 138 kJ mol^{-1} for samples with thicknesses of 0.55 and 0.98 mm at 900 °C [11], indicating that ceramics prepared from perovskite powders have higher oxygen permeation. It can be further concluded that the perovskite powders are suitable for preparing dense ceramics.

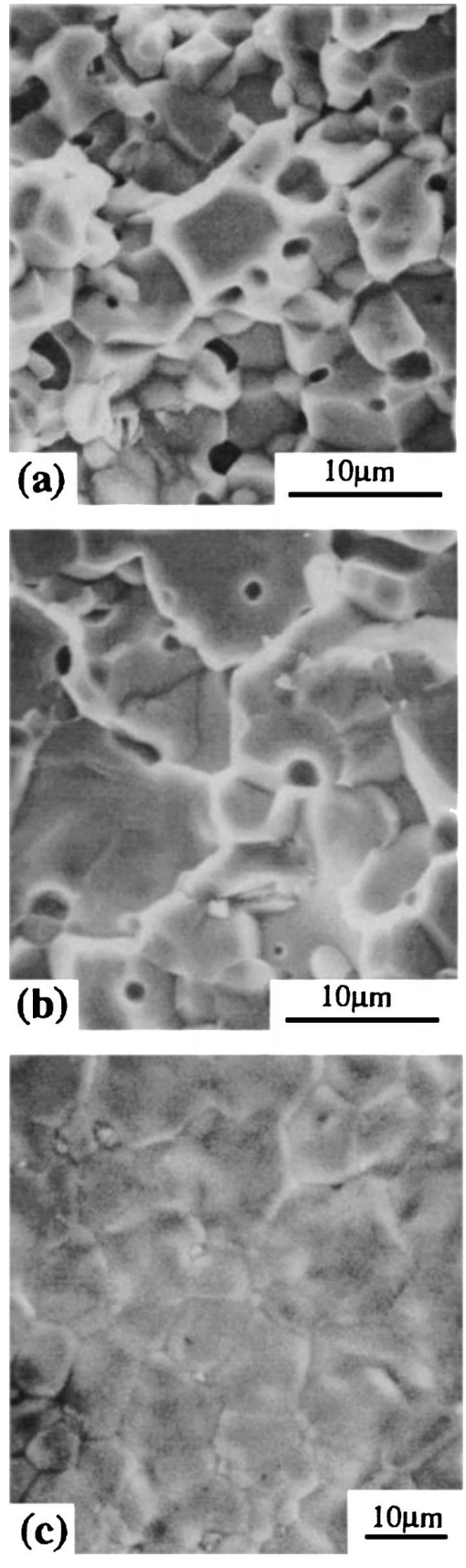

Figure 4 Scanning electron micrographs of perovskite ceramics by gelcasting sintered at different temperature for 6 h: (a) 1150 °C, (b) 1250 °C, and (c) 1300 °C.

4. Conclusions

Perovskite $La_{0.6}Sr_{0.4}Co_{0.8}Fe_{0.2}O_{3-\delta}$ powders have been synthesized from oxide and carbonate based on the principle of gelcasting. Phase-forming temperature is very dependent on the ball-milling process during preparation of the suspension. The perovskite powders have pure phase and good sinterability. The permeation

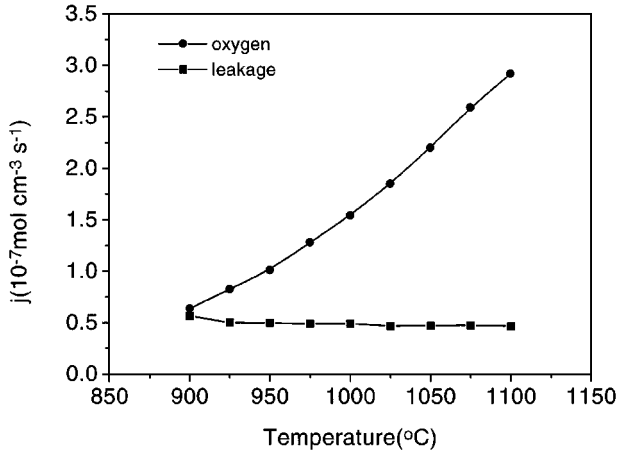

Figure 5 Oxygen permeance and leaked flow of disc LSCF samples versus temperature.

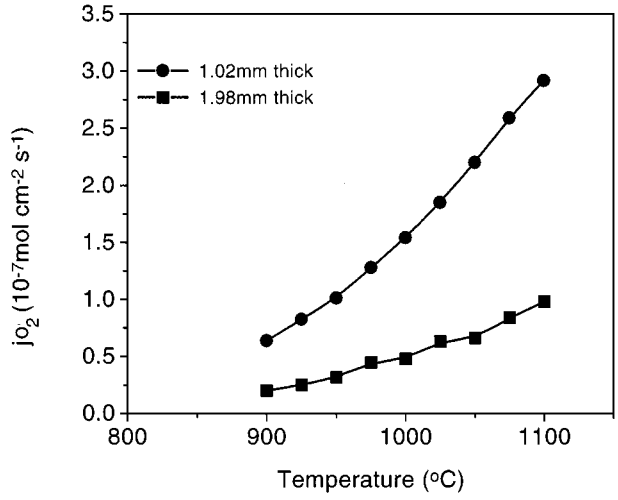

Figure 6 Temperature variation of the oxygen permeation rate from the air to the helium (35.92 cm^3 min^{-1}) side of disc LSCF samples (12 mm in diameter).

experiment shows disc-shaped samples fabricated from perovskite powders have high oxygen permeance. Consequently, it can be concluded that gelcasting is a simple and effective method for preparing practical multicomponent perovskite powders.

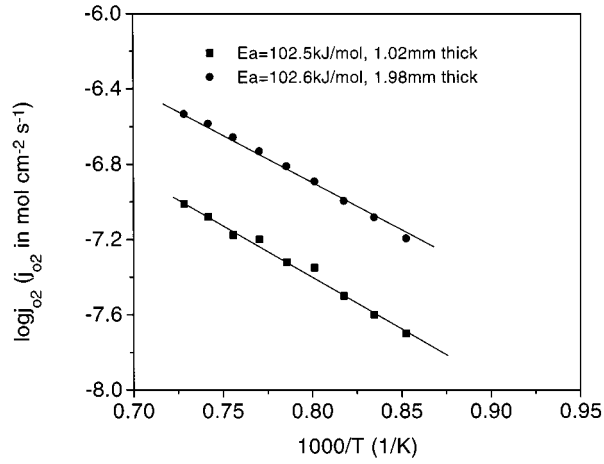

Figure 7 Plot of log jo_2 versus 1000/T transferred from Fig. 6.

Acknowledgements

The authors are grateful to the National Natural Science Foundation of China and the Natural Science Foundation of Anhui Province of China for financial support.

References

1. E. A. LOMBARDO and M. A. ULLA, *Res. Chem. Intermediat.*, **24** (1998) 581.
2. J. G. BEDNORZ and K. A. MULLER, *Z. Phys.* **B64** (1996) 189.
3. D. M. SMYTH, *Cryst. Latt. Def. Amorph. Mater*. **18** (1989) 355.
4. N. Q. MINH, *J. Amer. Ceram. Soc*. **76** (1993) 563.
5. YASUTAKE TERAOKA, HUA-MIN ZHANG, SHIOCHI FURUKAWA and NOBORU YAMAZOE, *Chem. Lett*. (1985) 1743.
6. K. VIDYASAGAR, J. GOPALAKRISHNAN and C. N. R. RAO, *J. Solid State Chem*. **58** (1985) 29.
7. F. H. CHEN, H. S. KOO and T. TSENG, *J. Amer. Ceram. Soc*. **75** (1992) 96.
8. S. BILGER, E. SYSKAKIS, A. NAOUMIDIS and H. NICKEL, *ibid*. **75** (1992) 4964.
9. O. O. OMATETE, M. A. JANNEY and R. A. STREKLOW, *Ceram. Bull*. **70** (1991) 1641.
10. H. T. WANG, X. Q. LIU, H. ZHENG, W. J. ZHENG and G. Y. MENG, *Ceram. Int.* in press.
11. J. E. TEN ELSHOF, PhD thesis, University of Twente, Enschede, The Netherlands (1997).

Received 21 July
and accepted 28 August 1998